Magnetic Response of Anisotropic Metal Fiber Material Using Homogeneous Technique in ECNDT

Article *in* IEEE Transactions on Magnetics · May 2007

DOI: 10.1109/TMAG.2007.892520 · Source: IEEE Xplore

Samir Bensaid
Université de Bouira

Gerard Berthiau
University of Nantes

Magnetic Response of Anisotropic Metal Fiber Material Using Homogeneous Technique in ECNDT

Vincent Doirat, Samir Bensaid, Javad Fouladgar, Gérard Berthiau, and Anthony Lefevre

CRTT-IREENA, 44600 Saint Nazaire, France

The 3-D shell elements model is used to determine the sensor impedance variation due to anisotropic metal fiber composite materials (AMFCM). The homogenization of these materials is realized by the inverse problem method. The impedance variation gives the information about the lift off and/or the integrity of the AMFCM.

***Index Terms*—Anisotropy, eddy currents, homogenization, nondestructive testing, shell elements.**

I. Introduction

The anisotropic metal fiber composite materials (AMFCM) allow to manufacture flexible and resistive structures used in automobile and nautical industries. They are made of several superimposed metallic fiber layers with different orientations as shown in Fig. 1. Due to their structure, these materials are nonisotropic and the study of their lift off or their integrity requires an anisotropic electromagnetic formulation.

Finite elements has been used to determine the stress inside nonisotropic structure [1]. In this paper, we propose to study the electromagnetic behavior of an AMFCM sheet. Our main contribution in this paper consists in taking into account of anisotropy in a shell element formulation. For that, we adapted a homogenization technique. We suppose that the excitation currents are sinusoidal with frequencies such that quasi-static approximation could be applied. The ability to simulate and anticipate the influence of composite materials on the sensor impedance is possible thanks to 3-D finite-elements modeling (3-D FEM). However, the great number of fibers in the AMFCM does not allow us to take into account the real geometry in the simulation. Homogenization techniques should, therefore, be used to evaluate the terms of equivalent conductivity tensor $\sigma_{\rm eq}$ and relative permeability tensor $\mu_{\rm eq}$ of the material [2]. Moreover, the thickness of the AMFCM is negligible with regard to the other dimensions. An anisotropic shell element formulation is consequently used to minimize the number of mesh elements [3], [4].

II. Homogenization of AMFCM

Various methods of homogenization can be used according to the studied structures: microscopic, macroscopic, or periodic [2]. In our case, the nonhomogeneous material studied possesses a microscopic regular anisotropy.

The inverse problem methodology is, therefore, used to calculate the homogeneous conductivity and relative permeability of the equivalent material. This method enables us to have the same active and reactive powers, be it in equivalent or in real materials.

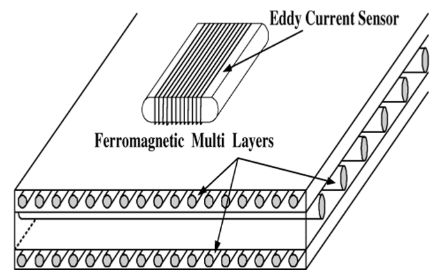

Fig. 1. EC NDT for anisotropic multilayers.

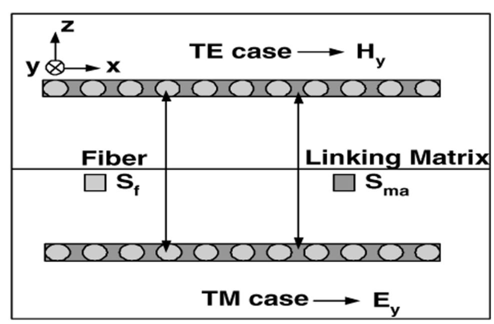

Fig. 2. TE and TM.

As in the electromagnetic wave propagation, two modes should be studied: transverse electric (TE), with magnetic field parallel to the fibers and transverse magnetic (TM) with electric field parallel to the fibers Fig. 2.

Fig. 3 shows the algorithm for the two homogeneous parameters. The inverse problem method searches the terms of $\sigma_{\rm eqfin}$ and $\mu_{r_{\rm eqfin}}$ by minimizing F. This objective function represents the difference between the active and the reactive powers of the real and equivalent materials. The Nelder and Mead Simplex algorithm is used to solve minimization problems [5].

We apply this homogenization process to a layer of n_f metallic fibers of radius R_f, electric conductivity σ, and relative permeability μ_r. The linking matrix is supposed to be nonconductor. The occupancy rate of the fibers with regard to the volume of material is noted τ. In the TE case, the equivalent

Digital Object Identifier 10.1109/TMAG.2007.892520

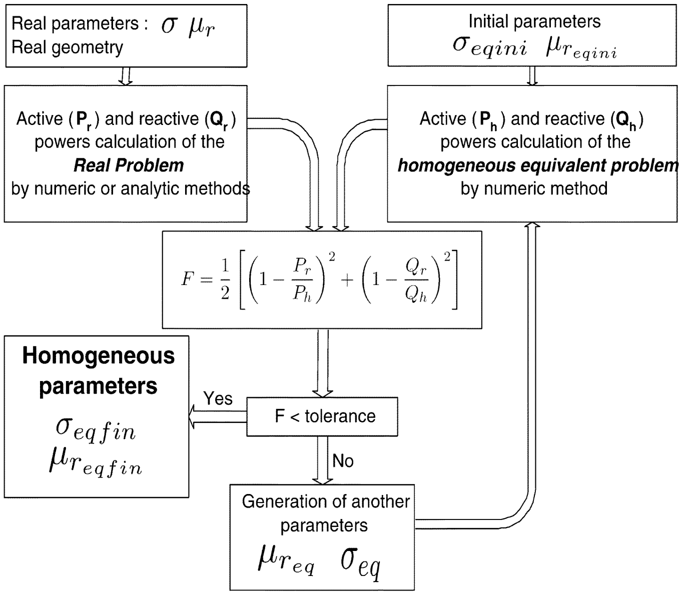

Fig. 3. Algorithm of homogeneous parameters calculation by power minimization.

relative permeability is weighted proportionally to the fibers and linking matrix volumes

$$\mu_{r_{\rm eq}} = \mu_r \tau + (1-\tau). \tag{1}$$

The active and reactive powers in the real material are analytically estimated. The eddy currents inside the fiber are calculated by Kelvin distribution for constant tangential magnetic field $\mathbf{H_0}$. The complex Poynting vector integral is then used to calculate the complex powers inside the fibers (S_{rf})

$$\mathbf{J} = \mathbf{H_0} k j^{1.5} \frac{J_0(kR_f j^{1.5})}{J_1(kR_f j^{1.5})} \tag{2}$$

$$P_{\rm poyn} = -n_f \oint_S \mathbf{E} \times \mathbf{H_0^*} {\rm d}S \tag{3}$$

$$S_{rf} = -n_f 2\pi R_f \mathbf{H_0^2} \sigma^{-1} k j^{1.5} \frac{J_0(kR_f j^{1.5})}{J_1(kR_f j^{1.5})}. \tag{4}$$

Moreover, the magnetic power stored in the linking matrix is

$$Q_{\rm rm} = j\,\omega\,\mu_0\,\mathbf{H_0^2}\,S_{\rm ma}. \tag{5}$$

The active and reactive powers in the composite are, respectively, the real and imaginary parts of S_r given by (6)

$$S_r = -n_f\,2\pi R_f\,\mathbf{H_0^2}\sigma^{-1} k j^{1.5} \frac{J_0(kR_f j^{1.5})}{J_1(kR_f j^{1.5})} + j\mu_0\omega \mathbf{H_0^2} S_{\rm ma} \tag{6}$$

where $k = \sqrt{j\,\omega\sigma\mu_0\mu_r}$, J_0 and J_1 are the zero- and first-order Bessel functions of first kind, ω is the angular frequency and $S_{\rm ma}$ is the surface of the linking matrix.

Active and reactive powers in the homogeneous material are estimated thanks to a 2-D FEM magnetic field formulation applied with equivalent conductivity and relative permeability.

The TM case is studied in the same way replacing μ by σ and using a 2-D FEM electric field formulation.

TABLE I
HOMOGENIZATION DATA

f	σ	μ_r
$10^3 \rightarrow 10^6$	$1.5MSm^{-1}$	200
Rf	nf	τ
$500\mu m$	50	from 20% to 80%

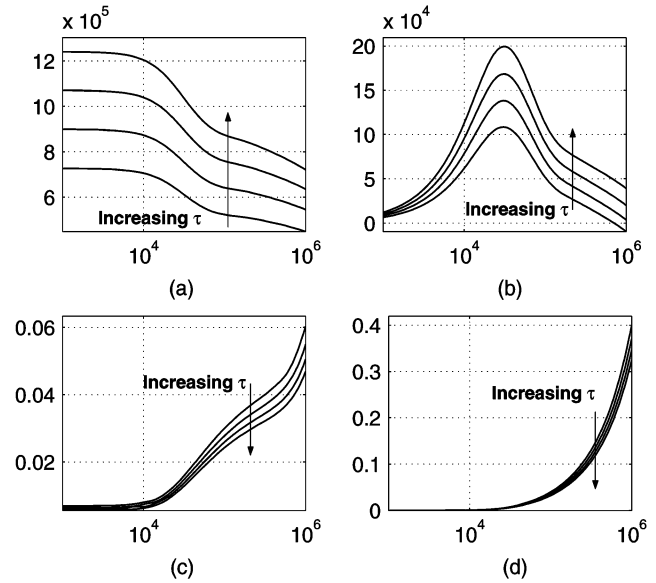

Fig. 4. (a,b) Equivalent conductivity and (c,d) equivalent relative reluctivity. (a) ${\rm Re}(\sigma_{\rm eq})$ versus Frequency. (b) -${\rm Im}(\sigma_{\rm eq})$ versus frequency. (c) ${\rm Re}(v_{\rm eq})$ versus frequency. (d) ${\rm Im}(v_{\rm eq})$ versus frequency.

To estimate the homogenization values, we have used the material characteristics shown in Table I.

Fig. 4(a) shows the variation of the real part and Fig. 4(b) shows the negative imaginary part of the equivalent conductivity in the TE case as a function of frequency. As mentioned before, the equivalent relative permeability depends on the occupancy rate τ. In this way, it is 80.6 for $\tau = 40\%$ and 160.2 for $\tau = 80\%$.

Fig. 4(c) shows the variation of the real part and Fig. 4(d) shows the imaginary parts of the equivalent relative reluctivity $(\nu_{r_{\rm eq}} = 1/\mu_{r_{\rm eq}})$ in the TM case. At the same time, the equivalent conductivity varies from $0.6MSm^{-1}$ (40%) to $1.2MSm^{-1}$ (80%).

Afterward, we note $\sigma_{\rm eq}$ and $\mu_{\rm eq}$ the equivalent conductivity and the equivalent relative permeability obtained thanks to the homogenization.

III. SHELL ELEMENT FORMULATION

The shell elements formulation has proven to be very efficient to reduce the number of nodes and the calculation time and has been used in the finite-element simulation of thin conducting regions [3]. An anisotropic shell element has been introduced in [4], to study the induction heating inside a carbon-fiber composite. Fig. 5 shows the schematic thin conducting plate with the tangential magnetic fields ($H_{1x}, H_{1y}, H_{2x}, H_{2y}$) and Fig. 6 shows the typical associated problem to be solved.

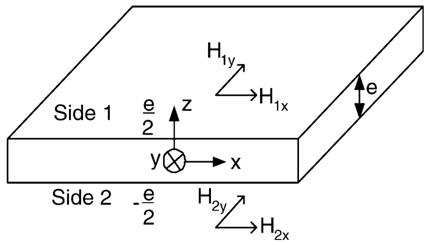

Fig. 5. Thin conducting plate.

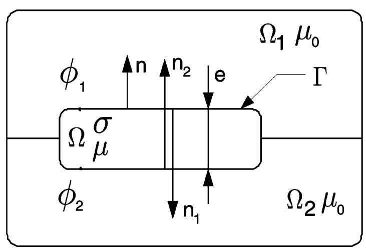

Fig. 6. General representation of shell elements.

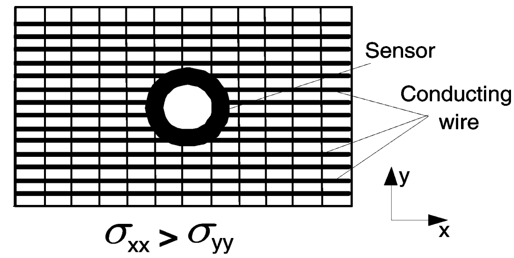

Fig. 7. Pancake above an anisotropic conductive plate with $\sigma_{xx} > \sigma_{yy}$.

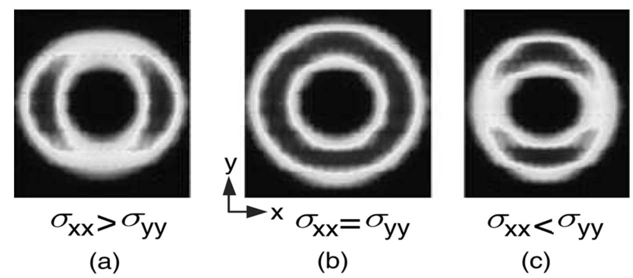

Fig. 8. Active power in an anisotropic plate.

The anisotropic electric conductivity and magnetic relative permeability tensors are introduced in electromagnetic equations. The electric conductivity is considered null in the plate in the $\mathbf{z}$ direction

$$\sigma_{\mathrm{eq}} = \begin{pmatrix} \sigma_{xx} & \sigma_{xy} & 0 \\ \sigma_{yx} & \sigma_{yy} & 0 \\ 0 & 0 & 0 \end{pmatrix} \tag{7}$$

$$\mu_{\mathrm{eq}} = \begin{pmatrix} \mu_{xx} & \mu_{xy} & 0 \\ \mu_{yx} & \mu_{yy} & 0 \\ 0 & 0 & \mu_z \end{pmatrix}. \tag{8}$$

As a consequence, the following coupled differential equations should be solved:

$$\begin{aligned} &\begin{cases} \frac{d^2 H_x(z)}{dz^2} + a * H_x(z) = b * H_y(z) \\ \frac{d^2 H_y(z)}{dz^2} + c * H_y(z) = d * H_x(z) \end{cases} \\ &a = -j\omega(\sigma_{yy}\mu_{xx} - \sigma_{yx}\mu_{yx}) \\ &b = j\omega(\sigma_{yy}\mu_{xy} - \sigma_{yx}\mu_{yy}) \\ &c = -j\omega(\sigma_{xx}\mu_{yy} - \sigma_{xy}\mu_{xy}) \\ &d = j\omega(\sigma_{xx}\mu_{yx} - \sigma_{xy}\mu_{xx}). \end{aligned} \tag{9}$$

The shell element formulation with reduced scalar potential ϕ on side "1" is written as

$$\begin{aligned} &\int_{\Omega_1} \mu\, \mathbf{grad}(w) \cdot \mathbf{grad}(\phi_1) d\Omega_1 \\ &\quad + \frac{1}{jw} \int_\Gamma \mathbf{grad}_s w \begin{bmatrix} -\alpha_1 & -\alpha_2 & \beta_1 & \beta_2 \\ -\alpha_3 & -\alpha_4 & \beta_3 & \beta_4 \end{bmatrix} \\ &\quad \times \begin{bmatrix} \mathbf{grad}_x(\phi_1) \\ \mathbf{grad}_y(\phi_1) \\ \mathbf{grad}_x(\phi_2) \\ \mathbf{grad}_y(\phi_2) \end{bmatrix} d\Gamma = \int_\Gamma \mu\, w\, \mathbf{H}_j . \mathbf{n}_1 d\Gamma \\ &\qquad - \frac{1}{jw} \int_\Gamma \mathbf{grad}_s w \begin{bmatrix} (\beta_1 - \alpha_1) & (\beta_2 - \alpha_2) \\ (\beta_3 - \alpha_3) & (\beta_4 - \alpha_4) \end{bmatrix} \\ &\qquad \times \begin{bmatrix} \mathbf{H}_{jx} \\ \mathbf{H}_{jy} \end{bmatrix} d\Gamma \end{aligned} \tag{10}$$

where $\alpha_{1,2,3,4}$ and $\beta_{1,2,3,4}$ are scalar coefficients depending on σ_{eq}, μ_{eq} and the angular frequency ω [4].

The other equation corresponding to the bottom side "2" of the plate is obtained by permuting the index 1 and 2 of normal vector $\mathbf{n}$ and reduced scalar potential ϕ in (10).

Once the reduced scalar potential is computed, we determine the magnetic and electric tangential field on both side of the composite

$$\begin{pmatrix} \mathbf{H_{1s}} \\ \mathbf{H_{2s}} \end{pmatrix} = \begin{pmatrix} \mathbf{H_{js}} - \mathbf{grad_s}(\phi_1) \\ \mathbf{H_{js}} - \mathbf{grad_s}(\phi_2) \end{pmatrix} \tag{11}$$

where $\mathbf{H_{js}}$ is the field calculated by Biot and Savart's law

$$\begin{bmatrix} E_{1x} \\ E_{1y} \\ E_{2x} \\ E_{2y} \end{bmatrix} = \mathbf{n} \times \begin{bmatrix} \alpha_1 & \alpha_2 & -\beta_1 & -\beta_2 \\ \alpha_3 & \alpha_4 & -\beta_3 & -\beta_4 \\ \beta_1 & \beta_2 & -\alpha_1 & -\alpha_2 \\ \beta_3 & \beta_4 & -\alpha_3 & -\alpha_4 \end{bmatrix} \begin{bmatrix} H_{1x} \\ H_{1y} \\ H_{2x} \\ H_{2y} \end{bmatrix}. \tag{12}$$

The active power injected inside the composite material is the real part of the Poynting vector integral. This power represents the resistance variation of the inductor if the skin and proximity effects in the inductor are neglected

$$\begin{aligned} P_{\mathrm{active}} = \frac{1}{2} \Bigg(&-\int\int_{S_1} (\mathbf{E_{1s}} \times \mathbf{H_{1s}^*}) \mathrm{d}S \\ &+ \int\int_{S_2} (\mathbf{E_{2s}} \times \mathbf{H_{2s}^*}) \mathrm{d}S \Bigg). \end{aligned} \tag{13}$$

The reactive power inside the plate and in free air represents the inductance of the sensor.

IV. Simulation and Measurement

A. Simulation

A circular sensor is placed above an anisotropic conductive plate (Fig. 7). The plate specific homogenized conductivity (σ_{xx} and σ_{yy}) has been estimated before hand.

Fig. 8 shows the active power in plate with different electrical conductivity values according to axes. This simulation shows

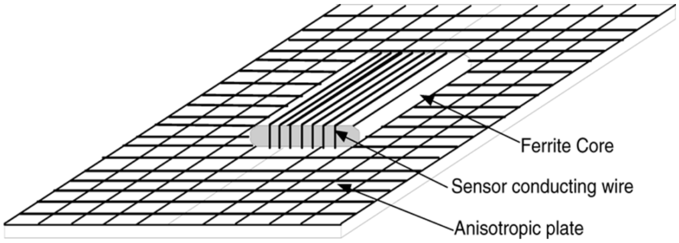

Fig. 9. Directive sensor to measure the lift off.

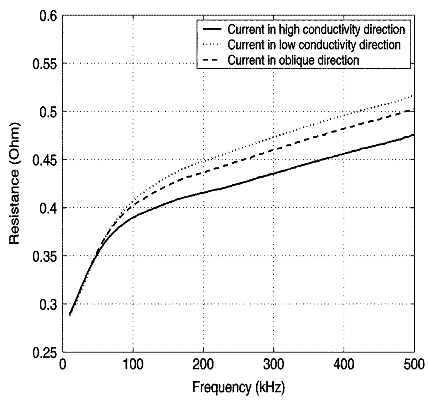

Fig. 10. Resistance variation versus frequency with anisotropic conductive plate.

that the active power is more important in the low conductivity direction. This is due to the fact that the eddy currents meet more resistance in this direction. So, the sensibility of the sensor depends on its orientation with regard to the conductivity. For resistance measurement, it is better to orient the induced current in the lower conductivity direction.

B. Measurement

Fig. 9 shows the sensor used to evaluate the lift off (distance between the sensor and the plate) of an anisotropic conductive plate. The impedance is measured by the "Agilent 4294A precision impedance analyzer." The sensor used directs the induced current according to a privileged direction.

Fig. 10 shows the resistance variation versus frequency for three directions. The measurements show that for frequencies lower than 100 kHz, the three curves are intermingled. Distinguishing the orientation of fibers is thus impossible with these frequencies. However, with more significant frequencies, it is possible to distinguish the orientation of fibers because the resistance is more important for the low conductivity direction as predicted by the simulation of Fig. 8.

Fig. 11 shows the resistance variation versus lift off for three directions. One observes the same result as in Fig. 10. The relative variation of resistance is about 70 mΩ per millimeter.

In a homogeneous material, not necessarily isotropic, if resistance increases the inductance decreases. It is not the case here as shown in Figs. 11 and 12. This phenomenon could be explained by the presence of capacities between the fibers of the material. In homogenization techniques, these capacities should be taken into account to obtain a more realistic equivalent material.

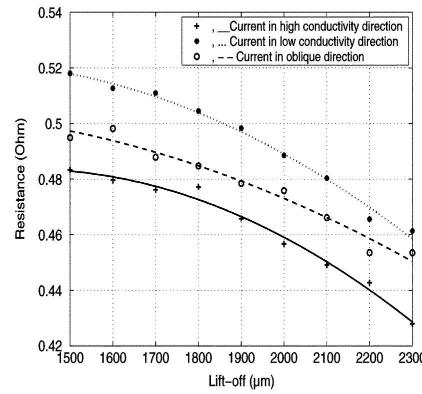

Fig. 11. Resistance variation versus lift off with anisotropic conductive plate.

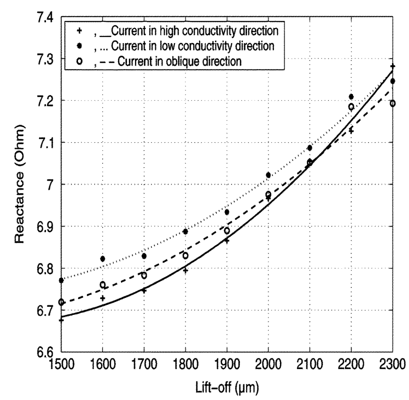

Fig. 12. Reactance variation versus lift off with anisotropic conductive plate.

V. Conclusion

The homogenization process has been developed from anisotropic material and has enabled us to get a homogeneous equivalent material. For this equivalent material, the shell element formulation has been adapted. The simulation with nonmagnetic, anisotropic material has proved that the active power injected is more important in the low conductivity direction. The sensibility of the resistance sensor depends on its orientation: the eddy currents induced by the sensor should be oriented in the low conductivity direction. In homogenization, capacities between the fibers of the material should be taken into account to obtain a more realistic equivalent material.

References

[1] C. C. Holt and D. Buttle, "Accuracy assessment of electromagnetic modelling of a stress measurement instrument," in *Proc. IEE Validation Comput. Electromagn. Seminar*, 2004, pp. 49–53.

[2] D. Trichet, J. Fouladgar, and G. Develey, "An estimator for equivalent properties of a bundle of conductors using the inverse problem method," *IEEE Trans. Magn.*, vol. 34, no. 5, pp. 2889–2892, Sep. 1998.

[3] C. Guérin, G. Tanneau, G. Meunier, P. Labie, T. Ngnegueu, and M. Sacotte, "A shell element for computing 3D eddy currents application to transformers," *IEEE Trans. Magn.*, vol. 31, no. 3, pp. 1360–1363, May 1996.

[4] S. Bensaid, D. Trichet, and J. Fouladgar, "3-D simulation of induction heating of anisotropic composite materials," *IEEE Trans. Magn.*, vol. 41, no. 5, pp. 1568–1571, May 2005.

[5] J. A. Nelder and R. Mead, "A simplex method for function minimization," *Comput. J.*, vol. 7, pp. 308–313, 1965.

Manuscript received April 24, 2006 (e-mail: vincent.doirat@univ-nantes.fr).